Received: 19 October 2022 | Revised: 20 January 2023 | Accepted: 2 February 2023

DOI: 10.1111/jnc.15778

Journal of Neurochemistry JNC The Official Journal of the International Society for Neurochemistry WILEY

ORIGINAL ARTICLE

NLRP3-directed antisense oligonucleotides reduce microglial immunoactivities in vitro

Charlotte Braatz[1] | Max P. Komes[1] | Kishore Aravind Ravichandran[1,2] | Matheus Garcia de Fragas[1,2,3] | Angelika Griep[1,2] | Stephanie Schwartz[1] | Róisín M. McManus[1,2] | Michael T. Heneka[1,4,5]

[1]Institute for Innate Immunity, University of Bonn, Bonn, Germany

[2]German Center for Neurodegenerative Diseases (DZNE), Bonn, Germany

[3]Department of Immunology, Institute of Biomedical Sciences, University of São Paulo, São Paulo, Brazil

[4]Department of Infectious Diseases and Immunology, University of Massachusetts Medical School, Worcester, Massachusetts, USA

[5]Luxembourg Centre for Systems Biomedicine, University of Luxembourg, Belvaux, Luxembourg

Correspondence
Michael T. Heneka, Luxembourg Centre for Systems Biomedicine (LCSB), University of Luxembourg, 6, Avenue du Swing, L-4367 Belvaux, Luxembourg.
Email: michael.heneka@uni.lu

Funding information
Alzheimer Forschung Initiative, Grant/Award Number: 20043; BONFOR research commission of the medical faculty of the University of Bonn, Grant/Award Number: 2021-4-06; Deutsche Forschungsgemeinschaft, Grant/Award Number: EXC2151 - 390873048; Deutscher Akademischer Austauschdienst, Grant/Award Number: scholarship

Abstract

Alzheimer's disease (AD) is associated with the cerebral deposition of Amyloid-β (Aβ) peptide, which leads to NLRP3 inflammasome activation and subsequent release of interleukin-1β (IL-1β) and interleukin-18 (IL-18). NLRP3 reduction has been found to increase microglial clearance, protect from synapse loss, and suppress both the changes to synaptic plasticity and spatial memory dysfunction observed in murine AD models. Here, we test whether NLRP3-directed antisense oligonucleotides (ASOs) can be harnessed as immune modulators in primary murine microglia and human THP-1 cells. NLRP3 mRNA degradation was achieved at 72 h of ASO treatment in primary murine microglia. Consequently, NLRP3-directed ASOs significantly reduced the levels of cleaved caspase-1 and mature IL-1β when microglia were either activated by LPS and nigericin or LPS and Aβ. In human THP-1 cells NLRP3-targeted ASOs also significantly reduced the LPS plus nigericin- or LPS plus Aβ-induced release of mature IL-1β. Together, NLRP3-directed ASOs can suppress NLRP3 inflammasome activity and subsequent release of IL-1β in primary murine microglia and THP-1 cells. ASOs may represent a new and alternative approach to modulate NLRP3 inflammasome activation in neurodegenerative diseases, in addition to attempts to inhibit the complex pharmacologically.

KEYWORDS
Alzheimer's disease, antisense oligonucleotides, Aβ, innate immunity, microglia, neuroinflammation, NLRP3 inflammasome

Abbreviations: AD, Alzheimer's disease; APP, amyloid precursor protein; Arg-1, arginase-1; ASC, apoptosis-associated speck-like protein containing a CARD; ASO, antisense oligonucleotide; Aβ, amyloid beta; BCA, bicinchoninic acid; CSF, cerebrospinal fluid; DAMP, damage-associated molecular pattern; DMEM, Dulbecco's modified Eagle's medium; DMSO, dimethyl sulfoxide; DPBS, Dulbecco's Phosphate Buffered Saline; EDTA, ethylenediaminetetraacetic acid; ELISA, enzyme-linked immunosorbent assay; EMA, European Medicines Agency; FBS, fetal bovine serum; FDA, Food and Drug Administration; IL-1β, interleukin-1 beta; IL-18, interleukin-18; LDH, lactate dehydrogenase; LPS, lipopolysaccharide; MM Con., mismatched control; NASH, non-alcoholic steatohepatitis; NF-κB, nuclear factor-κB; Nig., nigericin; NLRP3, NOD-, LRR-, and pyrin domain-containing 3; NOS2, nitric oxide synthase 2; NT Con., non-targeted control; PLL, poly-l-lysine; PMA, phorbol 12-myristate 13-acetate; PMO, phosphorodiamidate morpholino oligomers; PS, phosphorothioate; PS1, presenilin-1; P/S, penicillin/streptomycin; RIPA, ristocetin-induced platelet agglutination; RPMI, Roswell Park Memorial Institute 1640 Medium; RRID, Research Resource Identifier; Scr. Con., scrambled control; SMA, spinal muscular atrophy; TLR, toll-like receptor; TNF-α, tumor necrosis factor-alpha.

Róisín M. McManus and Michael T. Heneka contributed equally to this work.

1 | INTRODUCTION

Alzheimer's disease (AD) is the most common neurodegenerative disorder and cause of dementia, clinically characterized by the progressive loss of cognitive function and by behavioral changes (Reitz & Mayeux, 2014). It currently affects about 55 million individuals worldwide, likely increasing to 78 million by 2030 (Gauthier et al., 2021). The histopathological hallmarks of AD include the extracellular deposition of amyloid-β (Aβ) peptides, the intraneuronal formation of neurofibrillary tangles, and a concomitant innate immune activation. Aβ is cleavaged from amyloid precursor protein (APP) by two proteases, γ-secretase and β-secretase (Heneka et al., 2014). Aβ can be removed from the brain via export into the cerebrospinal fluid (CSF), known as glymphatic drainage, and is degraded by microglia (Heneka, Golenbock, & Latz, 2015) the major component of the brain's innate immune defense. Impaired clearance of Aβ can contribute to the development of sporadic AD (Mawuenyega et al., 2010).

Aβ is a danger-associated molecular pattern (DAMP), triggering neuroinflammation through the activation of pattern recognition receptors (PRRs) on microglia (Venegas et al., 2017; Weiner & Frenkel, 2006), which are heterogenous and may react in different ways to this challenge (Paolicelli et al., 2022). Mostly, however, the binding of a DAMP to a PRR activates the myeloid differentiation primary response protein MyD88 (MYD88)–nuclear factor-κB (NF-κB) pathway. As a result, the expression of the NOD-, LRR-, and pyrin domain-containing protein 3 (NLRP3) and the pro-form of the inflammatory cytokine interleukin-1β (pro-IL-1β) are upregulated (Halle et al., 2008; Heneka et al., 2018). A second signal is required to fully activate the NLRP3 inflammasome, where it undergoes a conformational change allowing the helical fibrillar assembly of an adaptor protein called apoptosis-associated speck-like protein containing a CARD (ASC) (Andreeva et al., 2021; Heneka et al., 2018; Hochheiser et al., 2022). Fibrillar ASC recruits caspase-1, which is then activated by autocatalysis and, in turn, cleaves and activates the pro-forms of IL-1β, IL-18, and gasdermin D (Boucher et al., 2018). Cleaved gasdermin D forms a pore in the outer cellular membrane, allowing movement of mature or active IL-1β and IL-18 to the extracellular space (Rathinam et al., 2019).

Protofibrils, oligomeric, and fibrillar Aβ all trigger NLRP3 inflammasome activation leading to significant release of mature IL-1β into the supernatant of primary murine microglia (Lučiūnaitė et al., 2020). In contrast, cells deficienct for NLRP3 (Halle et al., 2008) or use of the NLRP3-specific inhibitor CRID3 (Lučiūnaitė et al., 2020) protects microglia from the Aβ-induced production of cleaved caspase-1 and release of mature IL-1β. In vivo, NLRP3 knockout mice carrying APP/PS1 mutations were largely protected from Aβ deposition, immune activation of microglia, reduction in synaptic spines, and consequently spatial memory dysfunction (Heneka et al., 2013). The levels of cleaved caspase-1 and total IL-1β were significantly reduced in the brains of APP/PS1.NLRP3$^{-/-}$ mice in comparison with APP/PS1 mice and were instead on a par with age-matched wild-type controls (Heneka et al., 2013; Jankowsky et al., 2001).

As a result of these in vitro and in vivo findings, NLRP3 inflammasome inhibition is a promising therapeutic target for AD (Heneka et al., 2013). Indeed, a number of NLRP3 inhibitors are currently undergoing clinical trials for individuals with cryopyrin-associated autoinflammatory syndrome (CAPS), who have an overactive NLRP3 inflammasome. The results of these investigations will be relevant for all conditions where there is a NLRP3 inflammasome involvement, including AD. To date, IL-1β-pathway inhibitors such as anakinra or canakinumab are approved for therapeutic use (Dinarello et al., 2012), although their use in AD patients is not yet examined.

In contrast to pharmacological inhibition, protein expression can be modulated by antisense oligonucleotides (ASO). ASOs are short, synthetic, and single-stranded oligodeoxynucleotides that bind via complementary base pairing to their target mRNA. These RNA–DNA hybrids become substrates for RNase H, resulting in rapid mRNA degradation (Rinaldi & Wood, 2018).

Therapies with ASOs have been approved for neurological diseases including spinal muscular atrophy and Duchenne muscular dystrophy (Bennett et al., 2021). Indeed, there are a growing number of clinical trials examining the protectiveness of ASOs across a range of neurological diseases from amyotrophic lateral sclerosis, Huntington's disease, Parkinson's disease, and Angelman syndrome (Bennett et al., 2021; Scharner & Aznarez, 2021). In AD, ASOs that influence tauopathies by either blocking the synthesis of tau, or introducing alternative splicing to produce a less pathogenic tau protein are being investigated (DeVos et al., 2017; Schoch et al., 2016; Sud et al., 2014). Indeed, an ASO causing a RNaseH-mediated reduction in tau synthesis is already in a phase I/II clinical trial for patients with early-onset AD (Bennett et al., 2021).

In this current study, we investigate the effects of multiple self-designed NLRP3-directed ASOs in models of brain inflammation using primary murine microglia and human THP-1 cells. In both murine and human cells, we found that NLRP3-targeted ASOs successfully reduced the protein levels of NLRP3, thereby suppressing NLRP3 inflammasome activation and consequently IL-1β generation. Given the protective effect of silencing NLRP3 in models of AD (Heneka et al., 2013), together these findings highlight NLRP3-directed ASOs as a novel approach to reduce NLRP3 inflammasome signaling and prevent neuroinflammation in AD.

2 | MATERIALS AND METHODS

2.1 | Animals

All animals used for microglial cell isolation were treated according to the legal and ethical requirements of the University of Bonn—Medical Center (Germany). Mouse breeding and husbandry were approved by the veterinary office (Bonn, Germany) according to the German Animal Welfare Act. Adult mice were mated and pups of either sex were used for primary microglial

cell preparation. No ethics approval number was required or assigned by the institutional board for this kind of lethal experiments. Mice were housed at 22°C and with a 12 h light/dark cycle with free access to food and water. The procedures complied with the guidelines of animal welfare as laid down by the German Research Council (DFG). For this study, the brains of 287 P0 P0–P2, mixed-sex C57BL/6 N wild-type mice were used. The pups were sacrificed by decapitation.

2.2 | Oligonucleotide design, synthesis, and preparation

Folding of the homo sapiens and mus musculus NLRP3 mRNA into secondary or tertiary structures was analyzed by minimum free energy prediction using a tool of the ViennaRNA Web Services (http://rna.tbi.univie.ac.at/). Subsequently, a number of possible target sites were chosen that were predicted to be open and accessible for ASO binding (Table 1). The specific ASOs were analyzed for CpG motifs, secondary structure, and oligonucleotide dimer formation with the sequence calculator called OligoEvaluator™ provided by Sigma-Aldrich (http://oligoevaluator.com). Furthermore, all ASOs were checked for off-target hybridization by BLAST analysis. All ASOs were synthesized by Sigma-Aldrich. The ASOs used in this study were between 18 and 21 nucleotides in length, which are linked through a phosphorothioate (PS) backbone. The 5′- and 3′ ends consist of five 2′-O-(2-methoxy)ethyl-modified nucleotides. To eliminate ASO-specific effects scrambled (Scr. Con.) and mismatched (MM Con.), ASOs were used as controls. Oligonucleotide sequences were as follows. Underlined parts correspond to 2′-O-(2-methoxy) ethyl modifications.

TABLE 1 Sequence of human and mouse ASOs.

Oligo name	ASO sequence (5′-3′)
human ASO 1	GAUGCCATCTTGACCCAU
human ASO 2	GCUCCGGTGCTCCTTGAUGA
human ASO 3	CCCAGGCTCCTCTGUGUCA
human Scr. Con. 2	GUCUATCTCAGGTGGUCGCC
human MM Con. 2	GCUCCGGTATGAATTGAUGA
mouse ASO 1	ACUCUGGCTGGTCCTUCUUA
mouse ASO 2	AUCCACTCTTCTTCAAGGC
mouse ASO 3	UCCCAGTGCCCAGTCCAAC
mouse ASO 4	UCACUTCAATCCACUUCA
mouse Scr. Con. 3	AGCUCCGCGACTCCUACCA
mouse MM Con. 3	UCCCAGTATATCGTCCAAC
mouse Scr. Con. 4	ACCUCCACTATACUUCAU
mouse MM Con. 4	UCACUTCCGATAACUUCA
NT Con.	CCUCUTACCTCAGTTACAATUUAUA

2.3 | Study design

No randomization procedures were applied to this study. No preliminary sample calculation was performed. The sample size was estimated based on similar studies previously carried out in the laboratory (Lučiūnaitė et al., 2020). There were no pre-determined exclusion criteria. No blinding was applied in the cell culture treatment, or to the analysis.

2.4 | Cell culture

2.4.1 | Primary murine microglia

For this experiment, mice were housed for primary microglia cell preparation only which did not require further approval. Primary murine microglia were prepared from P0–P2, mixed-gender mouse pups. After removing the meninges, cells were separated with 0.25% trypsin and by mechanical shearing. Afterward, pooled cells were transferred into T75 culture flasks coated with Poly-L-Lysine (PLL). Primary murine microglia cells were cultured under standard conditions at 37°C and 5% CO_2 (1–2 brains per flask) in Dulbecco's modified Eagle's medium (DMEM, GIBCO) containing 10% heat-inactivated Fetal Bovine Serum (iFBS, GIBCO), 1% Penicillin/Streptomycin (P/S, GIBCO), and 1 mL of filtered L929 cell supernatant as a source for growth factors. After 24 h, flasks were washed three times with Dulbecco's Phosphate Buffered Saline (DPBS, GIBCO) and cultured for additional 7–10 days. When confluent, microglia were shaken off from the astrocyte monolayer. This was followed by two more shake cycles every second to third day.

2.4.2 | THP-1 cells

4×10^6 cells were cultured in Roswell Park Memorial Institute (RPMI) 1640 medium (GIBCO) containing 10% iFBS and 1% P/S at 37°C and 5% CO_2 atmosphere. THP-1 cells were passaged every 3–4 days, and 4×10^6 cells were cultured again. Passages ranged from p7 to p23.

2.5 | Cell transfection

For transfection, appropriate ASO concentrations from 1 to 300 nM were prepared. The ASOs (at various concentrations) or Dextran-488 (Invitrogen, 0.1 mg/mL final concentration) were mixed with lipofectamine RNAiMax (Invitrogen, final concentration, 0.3 μL/mL) and incubated at room temperature for 20 min. Subsequently, serum-free DMEM or RPMI medium was added to achieve the correct final concentration and volume. The ASOs were then added to the cells.

2.6 | Flow cytometry

Primary murine microglia or THP-1 cells were plated at 5×10^5 cells/well in a 12-well plate, in DMEM containing 1% P/S, 1% N-2 supplement (GIBCO) or in RPMI-1640 containing 1% P/S and 50 nM PMA, respectively. After 4–6 h the dextran/lipofectamine complexes were added to reach a final concentration of 0.1 mg/mL. Cells were incubated at 37°C for 3 h. The cells were gently scraped and incubated with LIVE/DEAD Aqua (Invitrogen). Fluorescence minus one served as controls. Flow cytometric analysis was performed on a BD FACSCanto II, and the data were acquired using Diva software (BD Biosciences). The flow cytometry results were analyzed using FlowJo software (TreeStar).

2.7 | Immunostaining and confocal microscopy

Primary microglia were plated onto PLL-coated coverslips at 3×10^5 cells/well and allowed to adhere overnight. The dextran/lipofectamine complexes were prepared as described above and added to the cells at a final concentration of 0.1 mg/mL. After 3 h, the cells were washed three times with PBS and then were fixed with 4% paraformaldehyde (PFA) in PBS for 15 min at room temperature. The cells were then washed again with PBS followed by nuclear counter-staining using Hoescht 33 342 (1:1000) in PBS + 0.1% Triton X100 for 15 min at room temperature. The coverslips containing the cells were washed with deionized water and were mounted onto glass slides using ProLong Gold Antifade reagent. Samples were dried in a cool dark place overnight. All the images were taken using 20X (air) objectives with the Zeiss LSM800 confocal microscope. Briefly, three regions of interest (ROIs) were imaged as a Z-stack per group. For the quantification and analysis, the maximum intensity Z-projections were used, all of which had undergone uniform brightness and contrast adjustments.

2.8 | Protein determination

To determine protein concentrations of cell lysates, a bicinchoninic acid (BCA) assay was performed using Pierce™ BCA Protein Assay Kit (Thermo Fischer Scientific) according to the manufacturer's protocol.

2.9 | Quantitative RT-PCR

Primary murine microglia were seeded at a density of 3×10^5 cells/well DMEM containing 1% P/S, 1% N-2 supplement in a 24-well plate. After 4–6 h the ASO/lipofectamine complexes were added to reach a final concentration between 1 and 300 nM. Cells were incubated at 37°C for 72 h with the ASOs.

THP-1 cells were seeded at a density of 6×10^5 cells/well in RPMI-1640 containing 1% P/S and 50 nM PMA in a 24-well plate, which was coated with Poly-L-Lysine (PLL). Again, after 4–6 h, the ASO/lipofectamine complexes were added to reach a final concentration between 1 and 300 nM. Cells were incubated at 37°C for 48 h with the ASOs.

RNA was extracted from the cells using miRNeasy Micro Kit following the manufacturers protocol (Qiagen). Total RNA was quantified spectrophotometrically, and 500 ng was reverse transcribed into complementary DNA using the High-Capacity RNA-to-cDNA™ Kit (Applied Biosystems™) according to the manufacturer's instructions. Real-time quantitative PCR was performed using the StepOnePlus Real-Time PCR System (Applied Biosystems). The TaqMan gene expression assay and TaqMan Universal PCR Master Mix (Applied Biosystems) were used for PCR amplification and real-time detection of PCR products. PCRs were performed in 20 µL with 2 µL of cDNA, 1 µL of each taqman probe, 10 µL of the master mix, and 6 µL of nuclease-free H_20 with the following temperature profile: 95°C for 10 min and 40 cycles of 95°C for 15 s and 60°C for 30 s. mRNA expression values were normalized to the internal level of 18S expression.

The following probes from LifeTechnologies were used: NLRP3 (Mm00840904_m1, Hs00918082_m1), PYCARD (Mm00445747_g1, Hs01547324_gH), Caspase-1 (Mm00438023_m1, Hs00354836_m1), IL-1β (Mm00434228_m1, Hs01555410_m1), TNFα (Mm00443258_m1, Hs00174128_m1), CD36 (Mm00432403_m1, Hs00354519_m1), CD68 (Mm03047343_m1, Hs00154355_m1), TLR2 (Mm00442346_m1, Hs00610101_m1), TLR4 (Mm00445273_m1, Hs00152939_m1), NOS-2 (Mm00440485_m1, Hs01075529_m1), Arginase-1 (Mm00475988_m1, Hs00163660_m1), IL-4 (Mm00445259_m1, Hs00174122_m1), IL-12 (Mm00434169_m1, Hs01073447_m1) and Gasdermin D (Mm00509957_m1, Hs00986748_g1).

Analysis of the expression of the genes was performed using StepOne 2.2 software provided by Applied Biosystems.

2.10 | Measurement of cytokine secretion

For cytokine secretion experiments, *primary murine microglia* were seeded at a density of 5×10^4 cells/well in DMEM containing 1% P/S, 1% N-2 supplement in a 96-well plate. After 4–6 h, the ASO/lipofectamine complexes were added to reach a final concentration of 30 nM. Cells were incubated at 37°C for 72 h with the ASOs.

THP-1 cells were seeded at a density of 8×10^4 cells/well in RPMI-1640 containing 1% P/S and 50 nM PMA in a 96-well plate, which was coated with PLL. Again, after 4–6 h the ASO/lipofectamine complexes were added to reach a final concentration of 30 nM. Cells were incubated at 37°C for 48 h with the ASOs.

After incubation with the ASOs, cells were primed with 100 ng/mL lipopolysaccharide (LPS) (InvivoGen) for 3 h. Subsequently, they were treated with either 10 µM nigericin (InvivoGen) for 45 min or 5 µM $A\beta_{1\text{-}42}$ (Bachem) or its buffer controls (DMSO) for 24 h. Afterward, IL-1β and TNF-α secretion was measured in cell supernatants using the mouse and human IL-1β/IL-1F2 and TNF-α DuoSet ELISA (R&D Systems) according to the manufacturer's protocols. The reaction was terminated by adding 2 N H_2SO_4, and the optical density was measured at 450 nm with a microplate reader (Infinite M200; Tecan). To determine cytokine concentrations, values were interpolated into the standard curve by linear regression using GraphPad Prism 9 (GraphPad Software).

2.11 | Cytotoxicity and cell viability assays

For cytotoxicity experiments, *primary microglia* and *THP-1 cells* were treated as described above. LDH release was measured in 50 µL supernatant using a cytotoxicity detection kit (Roche) according to the manufacturer's protocol. The reaction was stopped with 1 N HCl and absorbance was measured at 490 and 680 nm using a microplate reader (Infinite M200; Tecan).

2.12 | Immunoblotting

Primary murine microglia were seeded at a density of 1×10^6 cells/well in serum-free DMEM in a 6-well plate. After 4–6 h, the ASO/lipofectamine complexes at 30 nM were added. Cells were incubated at 37°C for 72 h with the ASOs.

THP-1 cells were seeded at a density of 2×10^6 cells/well in serum-free RPMI-1640 containing 50 nM PMA in a 6-well plate, which was coated with PLL. Again, after 4–6 h, the ASO/lipofectamine complexes at 30 nM 10X were added. Cells were incubated at 37°C for 48 h with the ASOs.

For inflammasome activation, cells were treated with LPS and nigericin or Aβ as described above. Subsequently, supernatants were collected for protein precipitation. Therefore, 500 µL methanol and 125 µL chloroform were added to 500 µL supernatant and vortexed briefly. After 5 min centrifugation at 15 000 *g*, the upper aqueous phase was removed and 500 µL methanol was added to the remainder. Again, samples were vortexed briefly and centrifuged at 15 000 *g* for 5 min. Supernatants were removed and pellets were dried for 20 min at room temperature. The pellets were then resuspended in 20 µL 2X loading buffer (106 mM Tris–HCL, 141 mM Tris base, 2% LDS, 10% glycerol, 0.51 mM EDTA (pH 8.5), 360 mM 1,4-Dithiothreit (DTT), and 5 mg/mL Orange G) and denatured at 95°C for 5 min in a thermocycler.

For lysate collection, cells were washed with PBS and 150 µL 1X ristocetin-induced platelet agglutination (RIPA) buffer (25 mM Tris–HCl (pH 7.5), 150 mM NaCl, 0.5% sodium desoxycholate, 1% NP-40, and 0.1% SDS) supplemented with 1X Protease/Phosphatase Inhibitor Cocktail (Cell Signaling Technology) were added for 20 min. Cells were then scraped of the well plate and centrifuged at 21 000 *g* at 4°C for 15 min. Cell lysates were also denatured at 95°C for 5 min in a thermocycler.

Samples were separated on a NuPAGE 4%–12% Bis-Tris Gel (Invitrogen) in NuPAGE MES or MOPS SDS Running Buffer (NP0002). The Trans-Blot Turbo™ Transfer System (Bio-Rad Laboratories) was used to blot the proteins on a 0.2 mm nitrocellulose membrane (Trans-Blot Turbo™ Transfer Pack, Bio-Rad Laboratories). Thereafter, membranes were blocked with 3% fatty acid-free bovine serum albumin (BSA) (Millipore) in Tris-buffered saline supplemented with Tween-20 (TBST) (10 mM Tris–HCl, 150 mM NaCl, 0.05% Tween-20, pH 8.0) for 30 min at RT.

NLRP3 was detected using antibody anti-NLRP3/NALP3 Cryo-2 (AdipoGen, RRID:AB_2490202), ASC using Anti-Asc AL177 (AdipoGen, RRID:AB_2490440), caspase-1 using antibodies Casp1 clone 4B4.2.1 (Genentech, gift from Genentech), and anti-caspase-1 (human) Bally-1 (AdipoGen, RRID:AB_2490257), IL-1β using GTX74034 (Genentech, RRID:AB_378141), Human IL-1 beta /IL-1F2 Antibody AF-201-NA (R&D Systems, RRID:AB_354387), and Mouse IL-1β/IL-1F2 AF-401-NA (R&D Systems, RRID:AB_416684), NOS-2 using antibody 610 329 (BD Transduction Laboratories, RRID:AB_397719) and α-Tubulin using antibody 62 204 (Invitrogen, RRID:AB_1965960). All primary antibodies were used at a dilution of 1:1000 in 3% BSA in TBST. Primary antibody signal was detected by secondary IRDye IgG (H + L) antibodies (1:10000, LI-COR Biotechnology, RRID:AB_2687553, RRID:AB_2651127, RRID:AB_2687825, RRID:AB_2651128, RRID:AB_2650427, RRID:AB_2814913). Proteins were then visualized with the Odyssey CLx Imaging System (LI-COR Biosciences) and quantified using Image Studio (LI-COR Biosciences).

2.13 | Phagocytosis of amyloid-β

For phagocytosis assay, *THP-1 cells* were seeded and treated with the ASOs in a black 96-well plate as described above. After 48 h of ASO treatment, fresh medium was added to the cells containing 0.25 µM TAMRA-Aβ (Eurogentec). After 4 h, medium was removed and absorbance was measured at 540 nm excitation and 585 nm emission using a microplate reader (Infinite M200; Tecan). Subsequently, Trypan blue 0.2% was added to extinguish any extracellular TAMRA signal and absorbance was again measured at 540 nm and 585 nm. Finally, nuclear stain was performed using H33342 and absorbance was measured at 360 nm excitation and 418 nm emission.

2.14 | Statistics

Data evaluation was performed using Graph Pad Prism 9 (GraphPad Software). Data are presented as Mean ± SEM. in all displayed diagrams. All data points refer to independent experiments where n indicates an independent cell culture preparation. For grouped datasets, one-way ANOVA was performed followed by a post hoc Tukey test. When only two groups were statistically analyzed, a two-tailed *t*-test was performed. Kolmogorov–Smirnov normality test was carried out to test whether the values come from a Gaussian distribution. In addition, Grubbs' test (alpha of 0.05) was performed to remove any significant outliers. Levels of significance are indicated as $^*p < 0.05$; $^{**}p < 0.01$; $^{***}p < 0.001$; $^{****}p < 0.0001$. Full statistical reports are provided in Supporting Information (Table S1).

3 | RESULTS

3.1 | ASOs reduce expression of NLRP3 by murine microglia

To determine the effects of targeted ASOs on the expression of NLRP3, we set out to design NLRP3-targeted ASOs that were likely to bind to NLRP3 mRNA. First, we examined the regions of NLRP3

that were predicted to be in an open, as opposed to folded, conformation based on their minimum free energy prediction (Figure 1a). Focusing on the open regions, we designed four NLRP3-targeting ASOs complementary to different regions of NLRP3 mRNA (Table 1). Native oligonucleotides are very susceptible to degradation by endo- and exonucleases, but various chemical modifications to the backbone can substantially improve oligonucleotide stability (Bennett & Swayze, 2010; Crooke et al., 2017; Patil et al., 2005; Rinaldi & Wood, 2018). To enhance our ASO stability, we used phosphorothioate (PS) modified antisense oligonucleotides containing five 2′-O-(2-methoxy)ethyl-modified nucleotides on the 5′- and 3′ ends. Murine microglia were transfected with one of four different ASOs in lipofectamine RNAiMax at concentrations ranging from 0 to 300 nM for 72 h (Figure 1a,b).

ASO 1 and ASO 2 did not significantly affect the levels of NLRP3 mRNA in microglial cells (Figure 1c,d). In contrast, compared with untreated cells, ASO 3 and ASO 4 reduced mRNA levels in a dose-dependent manner, starting at concentrations of 30 nM (Figure 1e,f). Indeed when treated with ASO 3, NLRP3 mRNA expression was reduced by up to 50% (Figure 1e). At a protein level, ASO 3 reduced the amount of NLRP3 by over 60% (Figure 1g,h). To determine the microglial transfection efficiency, we used labeled dextran as a control, similar to that described before (Raes et al., 2021) (Figure S1a–e). We combined the dextran-488 with lipofectamine and treated the cells with these complexes for 3 h. Interestingly, 50–82% of microglial cells had taken up the labeled liposomes, as detected by flow cytometry (Figure S1a,b) or by immunocytochemistry (Figure S1e).

In order to account for off-target effects triggered by the ASOs, we designed scrambled (Scr. Con.) and mismatched (MM Con.) sequences of ASO 3 (Gagnon & Corey, 2019). These controls have the same nucleotide composition, but critically, the order of the nucleotides differs. Again, the ASOs were administered at 30 nM for a period of 72 h. Compared with the scrambled and mismatched controls, the NLRP3-targeted ASO 3 significantly reduced the protein levels of NLRP3 in microglia (Figure 1g,h). Together, the data suggest that ASO 3 functions to inhibit the mRNA levels of NLRP3 in a sequence-specific manner. For all subsequent studies in murine cells, ASO 3 was used at a concentration of 30 nM.

3.2 | NLRP3-directed ASOs successfully reduce the cleavage of both caspase-1 and IL-1β in primary murine microglia

We next asked whether the ASO-induced downregulation of NLRP3 persists when assembly of the inflammasome is triggered. To this

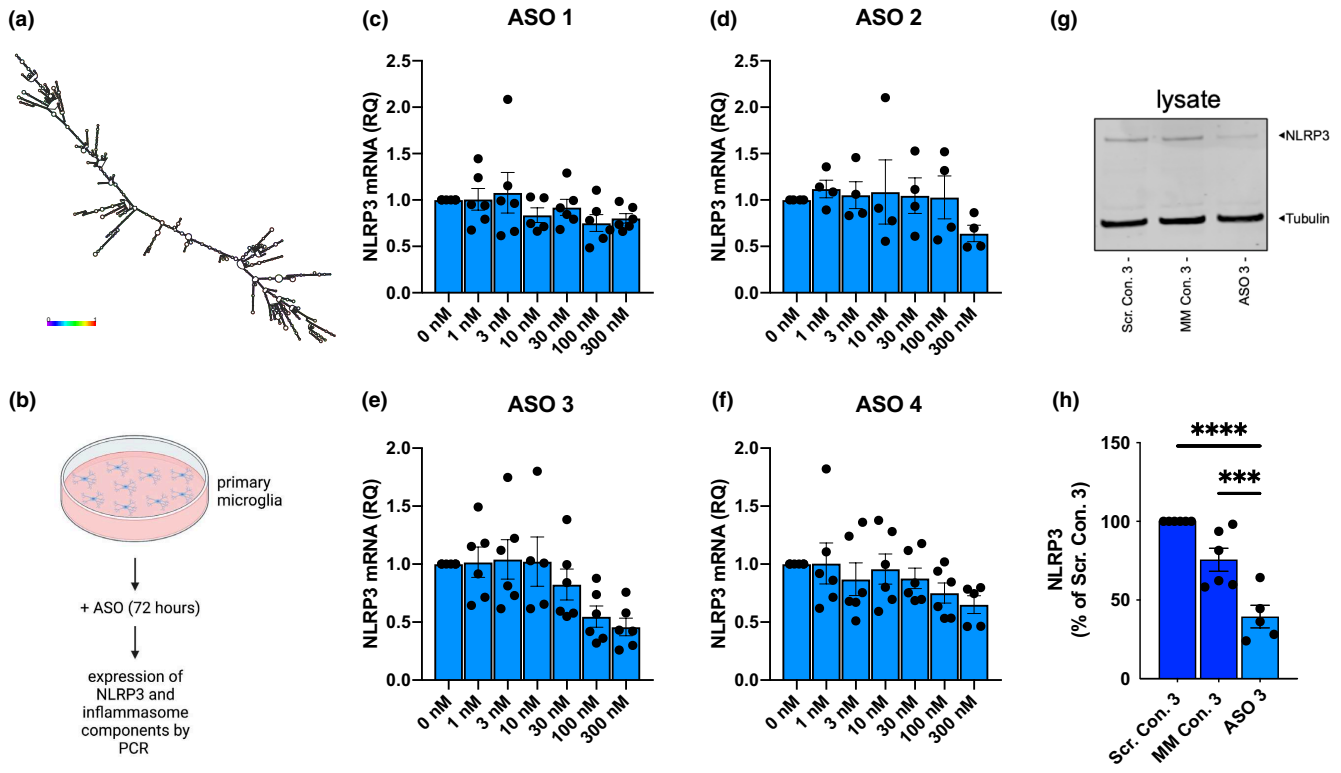

FIGURE 1 Development and characterization of murine NLRP3-targeted ASOs. (a) Minimum free energy prediction for mus musculus NLRP3 mRNA secondary structure colored by base-pairing probabilities. (b) Schematic of experimental setup. Microglia were treated with targeted or control ASOs for 72 h and subsequently harvested to detect the levels of NLRP3 mRNA and protein. (c–f) Transcription levels of NLRP3 in primary murine microglia treated with targeted ASOs for 72 h ($n = 6$ independent biological replicates, Mean ± SEM). (g and h) Western blot detection and quantification of NLRP3 in cell lysates of primary murine microglia treated with mouse ASO 3 and matching scrambled and mismatched controls at 30 nM for 72 h ($n = 6$ independent biological replicates, Mean ± SEM, one-way ANOVA, Tukey's post hoc test, ***$p < 0.001$, ****$p < 0.0001$). (Scr. Con. 3, scrambled control 3; MM Con. 3, mismatched control 3).

end, primary murine microglia cells were primed with lipopolysaccharide (LPS) and subsequently treated with nigericin (Figure 2a), which is an ionophore that permeabilizes the cell membrane to potassium and a well-known NLRP3-inflammasome activator (Mangan et al., 2018). Once the NLRP3 inflammasome is assembled, caspase-1 is recruited and undergoes autocatalysis, thus allowing it to cleave pro-IL-1β into active IL-1β (Heneka et al., 2018; Latz et al., 2013; Martinon et al., 2002). As expected, treatment with LPS and nigericin increased the expression of NLRP3 and pro-IL-1β in the cell lysates compared with an untreated control (Con) (Figure 2b,c, S2d), while the levels of pro-caspase-1 and ASC remained unchanged (Figure 2b, Figures S2a,c). Interestingly, prior treatment with NLRP3-targeted ASO 3, for 72 h, reduced the protein levels of NLRP3 and thus prevented inflammasome assembly (Figure 2b,c). In comparison, cells treated with the scrambled or mismatched ASO control maintained high levels of NLRP3 (Figure 2b–d, Figure S2b).

To determine the extent of inflammasome components released into the extracellular space, the cell supernatants were collected for ELISA and western blot analysis. As expected, all downstream NLRP3 inflammasome components including cleaved-IL-1β, cleaved caspase-1, and ASC were increased in the supernatant after stimulation with LPS and nigericin (Figure 2e–h, Figure S2e–g). Levels of pro-caspase-1 and pro-IL-1β released into the supernatant were reduced in tendency when compared to scrambled and mismatched controls. This phenomenon did not reach the level of statistical significance across all experiments, but nevertheless may indicate that because of the inhibition of the NLRP3 inflammasome, less microglial pyroptosis caused those reduced levels in the supernatant. (Figure 2e, Figure S2f,g). In contrast, NLRP3-directed ASO 3 significantly reduced the release of ASC, cleaved caspase-1, and mature IL-1β in comparison with cells that received the scrambled control (Figure 2e–h). ASO 3 also reduced the production of IL-1β in a concentration-dependent manner (Figure S1h). Compared with a matching scrambled control, 100 nM of targeted ASO treatment decreased extracellular IL-1β by 62%, whereas 30 nM still led to a significant reduction by 43% (Figure S1h). Indeed, the pro-inflammatory cytokine TNF-α remained unaffected by ASO treatment, confirming that identified changes were NLRP3-pathway specific (Figure S1i). To analyze the effects of ASOs on the viability of primary murine microglia, the release of lactate dehydrogenase (LDH) was measured as an indicator of cell death (Giordano et al., 2011). Compared with the scrambled control, there was no significant difference with ASO treatment, indicating that ASOs are not affecting cell viability (Figure S2j).

3.3 | NLRP3 expression is reduced after 48 h of NLRP3-targeted ASO treatment in THP-1 cells

To investigate the effects of targeted ASOs in human immune cells, we designed three ASOs complementary to different, open regions of human NLRP3 mRNA (Table 1, Figure 3a). The ASOs were tested in THP-1 cells, a human monocyte cell line, to model a human system in vitro. To create an experimental setup more similar to human microglia, the THP-1 cells were differentiated with phorbol 12-myristate 13-acetate (PMA) into macrophage cells (Balon & Wiatrak, 2021). The human NLRP3-targeted ASOs contained the same chemical modifications to the backbone as the murine-specific ASOs mentioned above in order to provide nuclease resistance. Again, to determine the extent of NLRP3 mRNA degradation, ASOs were administered at multiple concentrations ranging from 0 to 300 nM for 48 h (Figure 3b).

Similar to that observed in microglia, THP-1 cells rapidly took up the liposomes and approximately 50% of cells were transfected after just 3 h (Figure S1c,d). Treatment with all three ASOs led to a concentration-dependent reduction in NLRP3 mRNA expression at 48 h, compared with untreated cells (Figure 3c–e). However, this effect was not observed in ELISAs for the release of IL-1β. Compared with the non-targeted control (NT Con.), which was not specific for any of the three ASOs, only ASO 2 at 100 and 30 nM significantly reduced the IL-1β release that was triggered on exposure to LPS and nigericin (Figure S3a–d). This effect was concentration dependent, as 1 nM of ASO 2 did not affect cytokine release (Figure S3d). Therefore, as in primary microglia, a concentration of 30 nM was used for all subsequent studies. To confirm the effect of ASO 2 on NLRP3 expression, scrambled and mismatched sequences of ASO 2 were designed and used as controls. In comparison with the scrambled control, the NLRP3-targeted ASO 2 significantly reduced NLRP3 levels in cell lysates (Figure 3f,g).

3.4 | Targeted ASOs affect downstream activation of the NLRP3 inflammasome in human THP-1 cells after stimulation with LPS and Nigericin

To further assess the effects of NLRP3-directed ASOs in THP-1 cells, the NLRP3 inflammasome was primed and activated by incubating the cells with LPS and nigericin (Figure 4a). Treatment with a NLRP3-targeted ASO for 48 h prior to the immune stimulus significantly reduced NLRP3 inflammasome expression and subsequent caspase-1 cleavage in cell lysates compared with scrambled and mismatched ASO controls (Figure 4b–d). In contrast, levels of pro-caspase-1, ASC, pro-IL-1β, and IL-1β in the lysate remained unaffected (Figure 4b, S3e–h).

Stimulation with LPS and nigericin led to a significant release of all downstream inflammasome components, that is, active IL-1β, cleaved caspase-1, and ASC, into the extracellular space when compared to untreated controls (Figure 4e–h, Figure S3i,k). Interestingly, compared with matching scrambled and mismatched ASO controls, 48 h of targeted ASO treatment prior to inflammasome activation attenuated the release of NLRP3, cleaved caspase-1, and mature IL-1β to the supernatant (Figure 4e–h). In contrast, the amount of pro-caspase-1, pro-IL-1β, and ASC in the supernatant remained unchanged (Figure 4e, Figure S3i,k). These data indicate that NLRP3 mRNA degradation by targeted ASOs also decreases NLRP3-dependent recruitment and activation of caspase-1 in THP-1 cells,

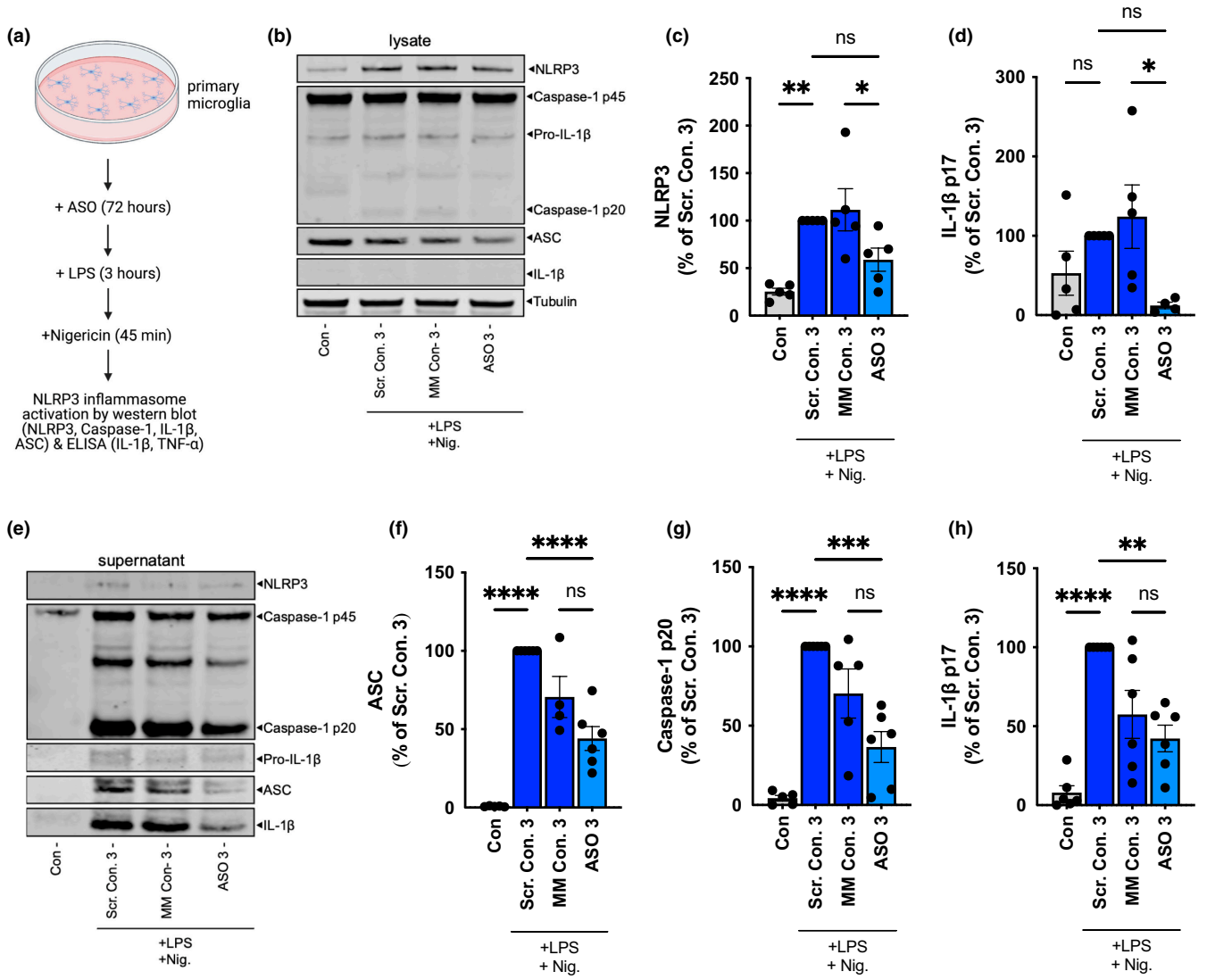

FIGURE 2 NLRP3-targeted ASOs protect against inflammasome activation and downstream release of cleaved caspase-1 and IL-1β in murine microglia. (a) Schematic of experimental setup. Microglia were treated with targeted or control ASOs for 72 h. Following this, the cells were incubated with LPS (100 ng/mL for 3 h) and then nigericin (10 μM for 45 min) and harvested to detect the levels of NLRP3 inflammasome-related components. (b–d) Western blot detection and quantification of NLRP3, caspase-1, ASC, and IL-1β in cell lysates of primary murine microglia that were treated with mouse ASO 3 and matching scrambled and mismatched controls at 30 nM for 72 h before stimulation with LPS and nigericin ($n = 5$ independent biological replicates, Mean ± SEM, one-way ANOVA, Tukey's post hoc test, $^{*}p < 0.05$, $^{**}p < 0.01$). (e–h) Western blot detection and quantification of NLRP3, caspase-1, ASC, and IL-1β in cell supernatants of primary murine microglia treated with mouse ASO 3 and matching scrambled and mismatched controls at 30 nM for 72 h before stimulation with LPS and nigericin ($n = 6$ independent biological replicates, Mean ± SEM, one-way ANOVA, Tukey's post hoc test, $^{*}p < 0.05$, $^{**}p < 0.01$, $^{***}p < 0.001$, $^{****}p < 0.0001$). (LPS, lipopolysaccharide; Nig., nigericin; Scr. Con. 3, scrambled control 3; MM Con. 3, mismatched control 3).

and consequently less IL-1β is released. This finding was further confirmed by ELISA, where the targeted ASO treatment reduced the extracellular levels of IL-1β compared with the matching scrambled control at all concentrations examined (Figure S3l). Indeed, 100 nM or 30 nM of NLRP3-targeted ASO 2 treatment significantly decreased extracellular IL-1β by 69% and 64% respectively (Figure S3l). TNF-α was undetectable in cell supernatants, which confirms NLRP3-dependency (Figure S3m). However, based on LDH release, targeted ASO treatment significantly reduced the LPS plus nigericin-induced cell toxicity (Figure S3n).

3.5 | ASO treatment significantly reduces IL-1β release in models of Aβ-induced inflammasome stimulation

To further study the protective effect of ASOs in the context of AD, we set up experimental paradigms using Aβ for inflammasome activation. Primary murine microglia and PMA-differentiated THP-1 cells received either murine- or human-specific NLRP3-directed ASOs and respective controls for up to 72 h. Subsequently, cells were primed with LPS for 3 h and inflammasome activation was

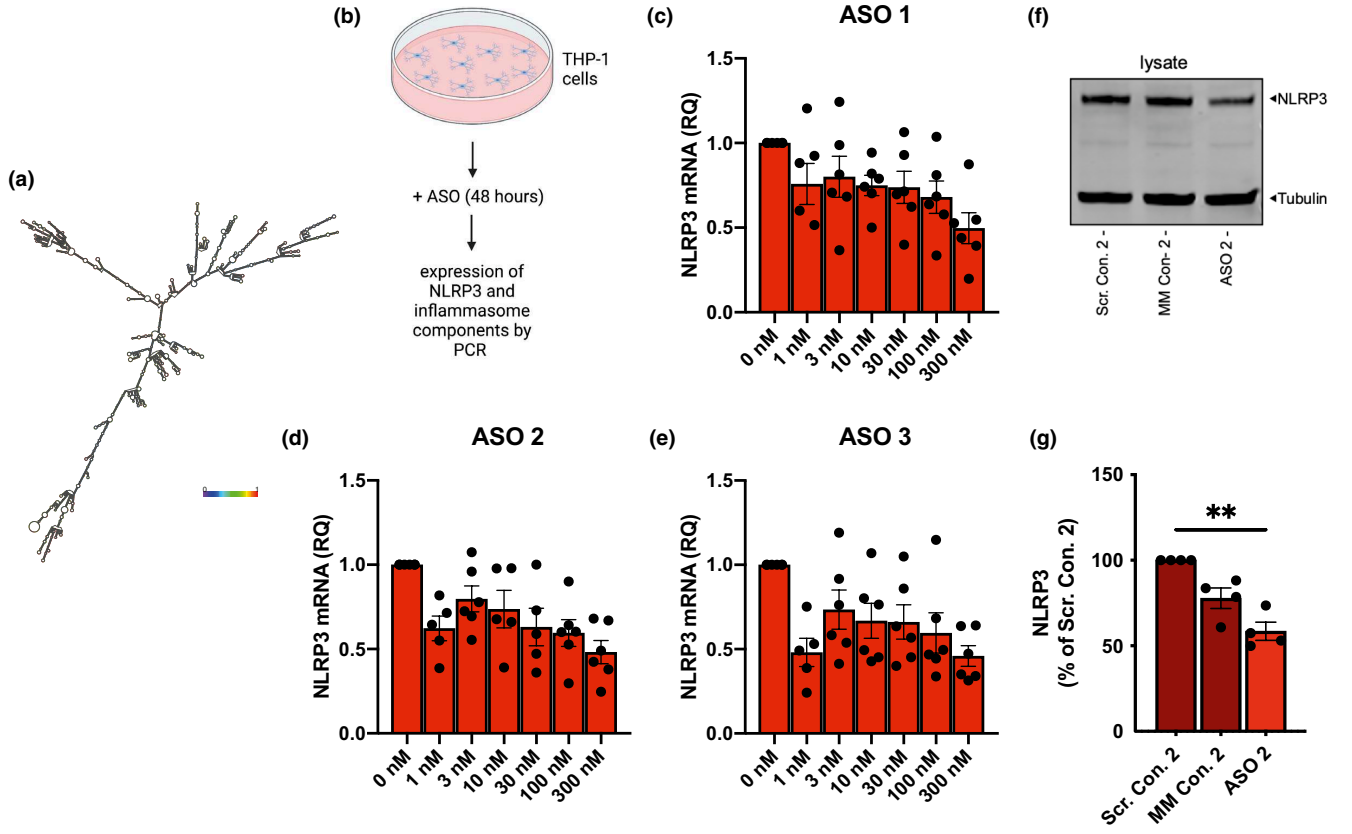

FIGURE 3 Characterization of human NLRP3-targeted ASOs. (a) Minimum free energy prediction for homo sapiens NLRP3 mRNA secondary structure colored by base-pairing probabilities. (b) Schematic of experimental setup. PMA-differentiated THP-1 cells were treated with targeted or control ASOs for 48 h and subsequently harvested to detect the levels of NLRP3 mRNA and protein. (c–e) Transcription levels of NLRP3 in THP-1 cells treated with targeted ASOs for 48 h ($n = 6$ independent biological replicates, Mean ± SEM one-way ANOVA, Tukey's post hoc test). (f and g) Western blot detection and quantification of NLRP3 in cell lysates of THP-1 cells treated with human ASO 2 and matching scrambled and mismatched controls at 30 nM for 48 h ($n = 4$ independent biological replicates, Mean ± SEM, one-way ANOVA, Tukey's post hoc test, $^{**}p < 0.01$). (Scr. Con. 2, scrambled control 2; MM Con. 2, mismatched control 2).

triggered by 24 h of Aβ exposure (Figure 5a). In primary murine microglia, Aβ increased IL-1β release compared with the DMSO control, which was used as a solvent (Figure 5b). This phenomenon was prevented by targeted ASO treatment and reduced IL-1β release from primary murine microglia by 68% (Figure 5b). TNF-α and LDH levels remained unaffected (Figure S4a,b). In our human model, NLRP3-targeted ASO 2 was similarly able to attenuate the Aβ-induced IL-1β release in THP-1 cells (Figure 5c). ASO 2 did not affect TNF-α and LDH release from these cells (Figure S4c,d). To further investigate the Aβ-induced recruitment and extracellular release of inflammasome components in primary murine microglia, immunoblot detection was performed. Treatment with a NLRP3-targeted ASO for 72 h decreased NLRP3 levels in cell lysates compared with the scrambled and mismatched control ASOs (Figure 5d,e). In contrast, the expression levels of ASC, pro-caspase-1, and pro-IL-1β remained unchanged (Figure 5d, Figure S4e–g). Additionally, immunoblot detection of cell supernatants revealed a significant reduction in cleaved caspase-1 and mature IL-1β in response to targeted ASO treatment (Figure 5f–i), while the release of NLRP3, ASC, pro-caspase-1, and pro-IL-1β were not affected (Figure 5f,g, Figure S4h–j).

3.6 | ASO treatment shifts murine microglia and human THP-1 cells toward an anti-inflammatory state

Microglial activation by pro-inflammatory stimuli causes a wide range of phenotypic changes that include increased expression of the inducible nitric oxide synthase 2 (NOS2). NOS2 is a hallmark of the classically activated pro-inflammatory phenotype, where it has previously been documented in the context of AD and linked to accelerated Aβ aggregation (Kummer et al., 2011). In contrast, arginase-1 represents a marker of an anti-inflammatory microglial phenotype (Heneka et al., 2013). Based on these markers, it has been shown that NLRP3-deficiency in APP/PS1 mice results in a phenotype shift toward an anti-inflammatory state (Heneka et al., 2013). In the present experiments, 72 h of NLRP3-targeted ASO treatment significantly down-regulated NOS2 mRNA levels in murine microglia, whereas arginase-1 mRNA was upregulated compared with untreated controls (Figure 6b,c). A trend toward increased arginase-1 expression was also observed in ASO 3 treated cells, in comparison with scrambled and mismatched ASOs (Figure 6d,e). Similarly, NOS2 mRNA was decreased by NLRP3-targeted ASO treatment in PMA-differentiated

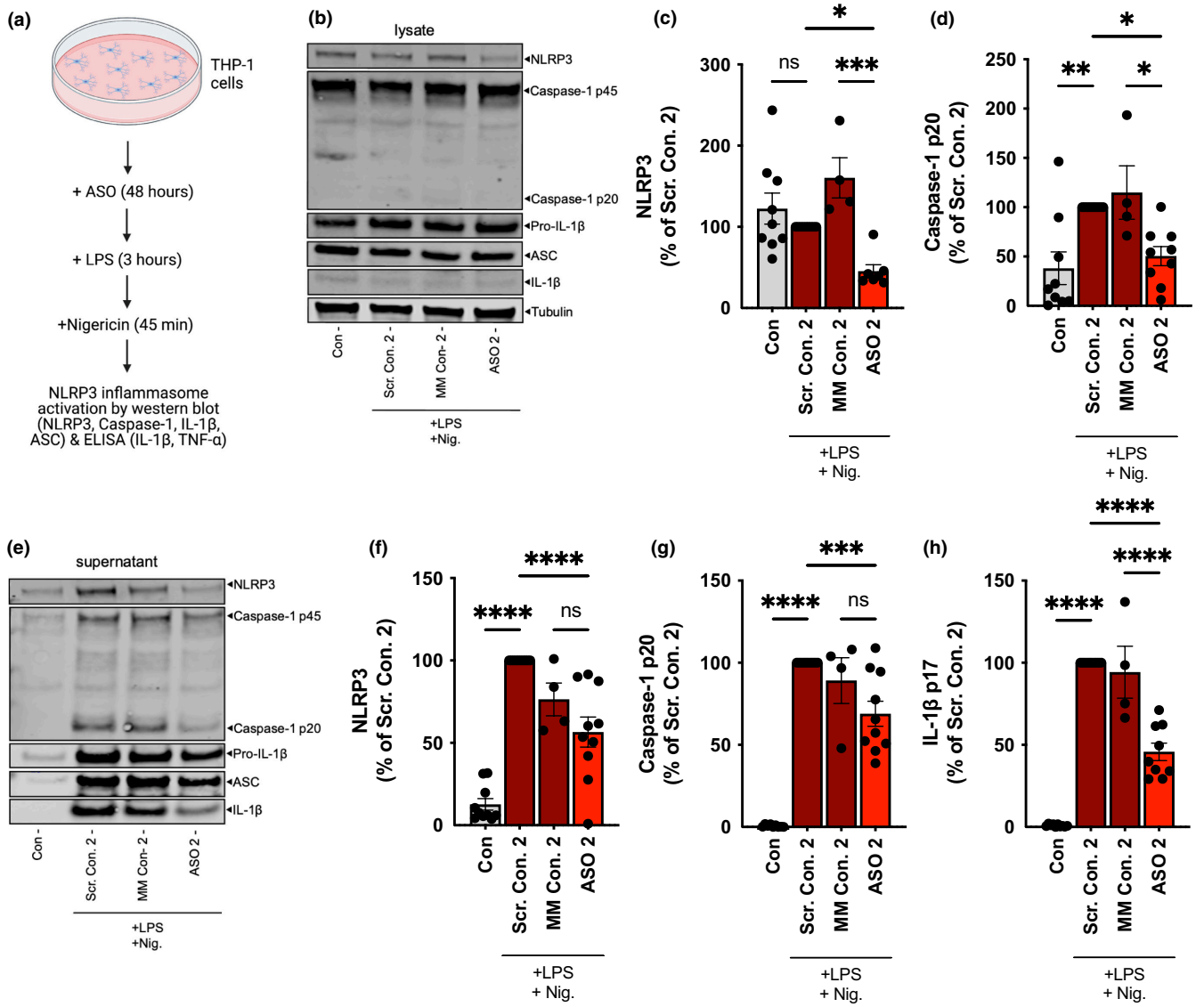

FIGURE 4 NLRP3-targeted ASOs prevent the LPS and nigericin-induced inflammasome activation in human cells. (a) Schematic of experimental setup. PMA-differentiated THP-1 cells were treated with targeted or control ASOs for 48 h. Following this, the cells were incubated with LPS (100 ng/mL for 3 h) and then nigercin (10 μM for 45 min) and harvested to detect the levels of NLRP3 inflammasome-related components. (b–d), Western blot detection and quantification of NLRP3, caspase-1, ASC, and IL-1β in cell lysates of THP-1 cells that were treated with human ASO 2 and matching scrambled and mismatched controls at 30 nM for 48 h before stimulation with LPS and nigericin ($n = 5$ independent biological replicates, Mean ± SEM, one-way ANOVA, Tukey's post hoc test, $^{*}p < 0.05$, $^{**}p < 0.01$, $^{***}p < 0.001$). (e–h) Western blot detection and quantification of NLRP3, caspase-1, ASC, and IL-1β in cell supernatants of THP-1 cells treated with human ASO 2 and matching scrambled and mismatched controls at 30 nM for 48 h before stimulation with LPS and nigericin ($n = 6$ independent biological replicates, Mean ± SEM, one-way ANOVA, Tukey's post hoc test, $^{*}p < 0.05$, $^{**}p < 0.01$, $^{***}p < 0.001$, $^{****}p < 0.0001$). (LPS, lipopolysaccharide; Nig., nigericin; Scr. Con. 2, scrambled control 2; MM Con. 2, mismatched control 2).

THP-1 cells, whereas arginase-1 levels were elevated although not significantly (Figure 6g,h). These experiments suggest that NLRP3 inflammasome activation and subsequent release of IL-1β act upstream of NOS2 expression. Consequently, mRNA degradation by NLRP3-directed ASOs reduces the expression of this pro-inflammatory enzyme. We next asked whether the suggested phenotype shift by NLRP3-directed ASOs also modifies microglial clearance capacity. The mRNA levels of CD68, which plays a key role in Aβ phagocytosis, were measured (Daria et al., 2017; Yamanaka et al., 2012). In both models, NLRP3-targeted ASO treatment significantly increased the amount of CD68 mRNA (Figure 6a,f). This was mirrored by a modest, but significant, increase in phagocytosis of TAMRA-labeled Aβ by ASO 2-treated THP-1 cells (Figure 6i,j).

4 | DISCUSSION

Aβ-triggered activation of the microglial NLRP3 inflammasome is a key driver of AD pathogenesis, where NLRP3 deficiency in APP/PS1 mice almost completely prevented the development of spatial memory

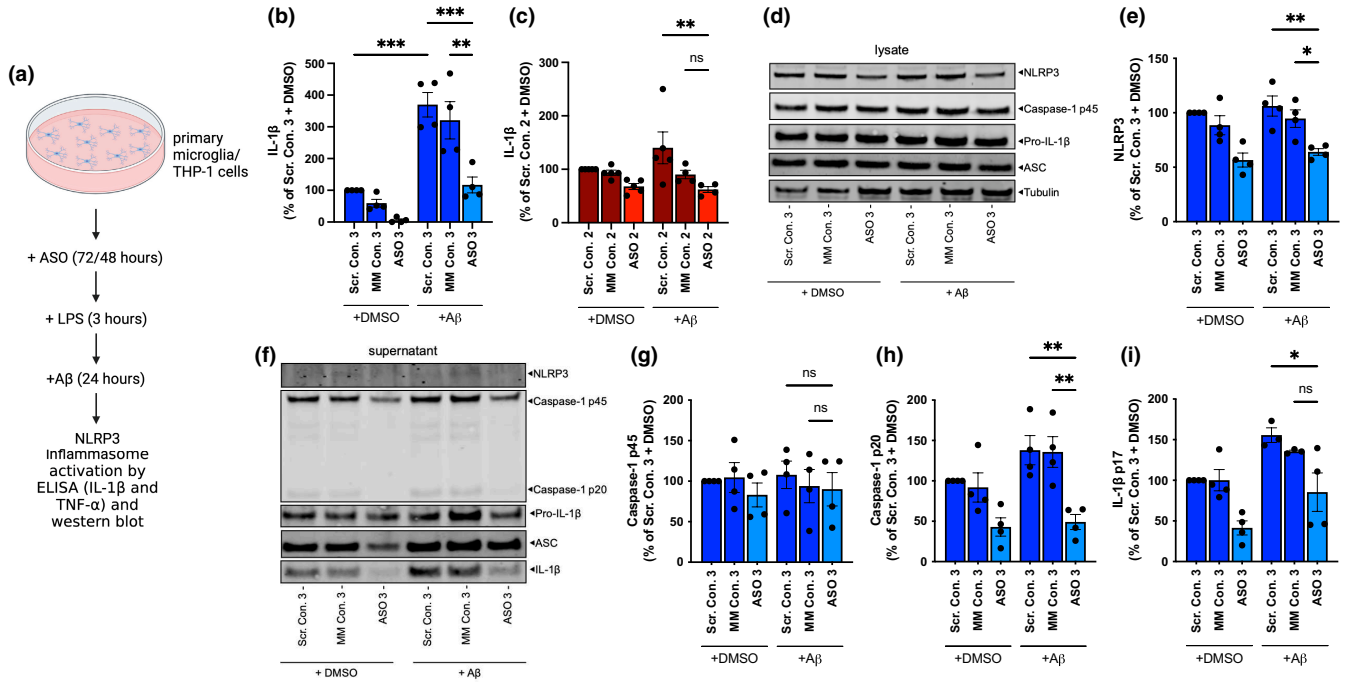

FIGURE 5 NLRP3-targeted ASOs attenuate Aβ-induced inflammasome activation, reducing IL-1β release. (a) Schematic of experimental setup. Microglia or THP-1 cells were treated with targeted or control ASOs for 72 or 48 h, respectively. Following this, the cells were incubated with LPS (100 ng/mL for 3 h) and then Amyloid-β (Aβ, 5 μM for 24 h). Following this, the cells were harvested to detect the levels of NLRP3 inflammasome-related components. (b) ELISA detection of IL-1β in cell supernatants of primary murine microglia that were treated with mouse ASO 3 and matching scrambled and mismatched controls at 30 nM for 72 h and then stimulated with LPS and Aβ ($n = 4$ independent biological replicates, Mean ± SEM, one-way ANOVA, Tukey's post hoc test, $^{*}p < 0.05$, $^{**}p < 0.01$, $^{***}p < 0.001$). (c) ELISA detection of IL-1β in cell supernatants of THP-1 cells treated with human ASO 2 and matching scrambled and mismatched controls at 30 nM for 48 h before stimulation with LPS and Aβ ($n = 4$ independent biological replicates, Mean ± SEM, one-way ANOVA, Tukey's post hoc test, $^{*}p < 0.05$, $^{**}p < 0.01$). (d–e), Western blot detection and quantification of NLRP3, pro-caspase-1, ASC, and pro-IL-1β in cell lysates of primary murine microglia treated with mouse ASO 3 and matching scrambled and mismatched controls at 30 nM for 72 h and then stimulated with LPS and Aβ ($n = 4$ independent biological replicates, Mean ± SEM, one-way ANOVA, Tukey's post hoc test, $^{*}p < 0.05$, $^{**}p < 0.01$). (f–i) Western blot detection and quantification of NLRP3, caspase-1, ASC, and IL-1β in cell supernatants of primary murine microglia treated with mouse ASO3 and matching scrambled and mismatched controls at 30 nM for 72 h and then stimulated with LPS and Aβ ($n = 4$ independent biological replicates, Mean ± SEM, one-way ANOVA, Tukey's post hoc test, $^{*}p < 0.05$, $^{**}p < 0.01$). (Aβ, amyloid-β; LPS, lipopolysaccharide; DMSO, dimethyl sulfoxide; Scr. Con. 3, scrambled control 3; MM Con. 3, mismatched control 3; Scr. Con. 2, scrambled control 2; MM Con. 2, mismatched control 2).

deficits (Heneka et al., 2013). Here, using primary murine microglia cells and human THP-1 cells, we tested whether ASOs would be able to directly target this inflammatory pathway in vitro under different protocols of NLRP3 inflammasome stimulation. After 72 h of targeted ASO treatment, NLRP3 mRNA degradation was successfully observed in primary murine microglia, and this downregulation persisted even when assembly of the inflammasome was triggered with LPS and nigericin (Pétrilli et al., 2007). Treatment with NLRP3-targeted ASOs resulted in a significant reduction in caspas-1 cleavage and IL-1β maturation, and prevented subsequent extracellular release of IL-1β compared with controls. Together, these data suggest that NLRP3-targeted ASOs in vitro can mimic the overall effects of a genetic NLRP3 knockout.

To further confirm the effects of NLRP3-targeted ASOs in the context of AD, we subsequently tested them using in vitro models of Aβ-induced inflammasome stimulation (Schnaars et al., 2013). In primary murine microglia, the Aβ-induced NLRP3 inflammasome activation and subsequent release of cleaved caspase-1 and mature IL-1β were prevented by targeted ASO treatment. In the human THP-1 cell model, reduced release of mature IL-1β was also observed with NLRP3-ASOs. Together, these data indicate that NLRP3 mRNA degradation by targeted ASO treatment reduces microglial inflammation in in vitro models.

As the progression of AD is not only based on Aβ pathology, the ASO-mediated effects might be because of other mechanisms not described here. Inflammasome-dependent formation and extracellular release of ASC specks also results in spreading of Aβ pathology in APP/PS1 mice (Venegas et al., 2017). In our in vitro murine model, NLRP3-targeted ASO treatment was shown to suppress the extracellular release of ASC specks (Figure 2f), which may also reduce or even prevent the subsequent ASC-dependent progression of Aβ plaque formation. Furthermore, deficiency of NLRP3 in Tau22 mice reduces tau hyperphosphorylation and aggregation by regulating tau kinases and phosphatases (Ising et al., 2019). Therefore, tau pathology could also potentially benefit from a NLRP3-targeted ASO therapy.

Previous studies have shown that NLRP3-deficiency in mice results in a microglial phenotype shift toward an anti-inflammatory

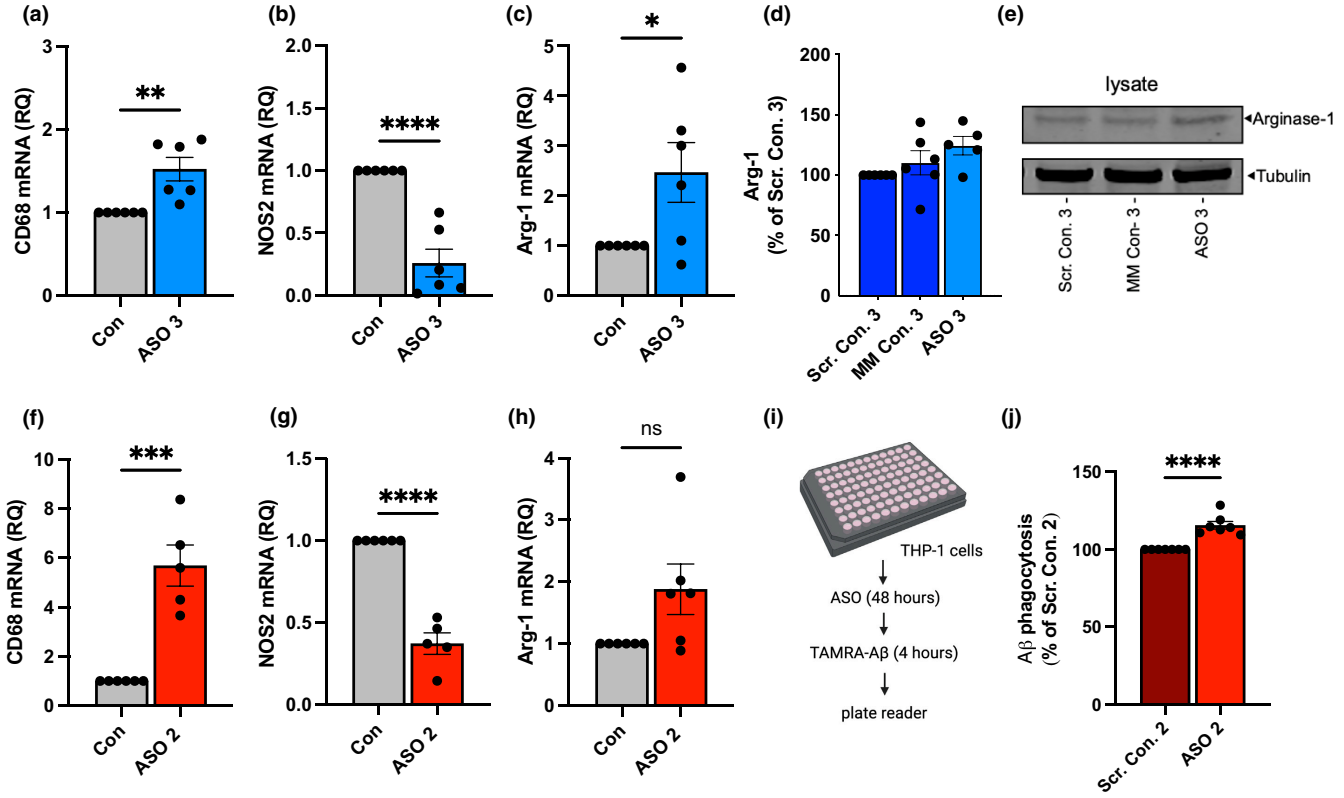

FIGURE 6 Transcriptional levels of anti-inflammatory and phagocytic genes increase after exposure to NLRP3-targeted ASOs. (a–c) Transcription levels of CD68, NOS2, and Arg-1 in primary murine microglia after 72 h of targeted ASO treatment at 30 nM ($n = 6$ independent biological replicates, Mean ± SEM, unpaired *t*-test, $^{*}p < 0.05$, $^{**}p < 0.01$, $^{***}p < 0.001$, $^{****}p < 0.0001$). (d and e) Western blot detection and quantification of arginase-1 in cell lysates of primary murine microglia that were treated with mouse ASO 3 and matching scrambled and mismatched controls at 30 nM for 72 h ($n = 6$ independent biological replicates, Mean ± SEM). (f–h) Transcription levels of CD68, NOS2, and Arg-1 in THP-1 cells after 48 h of targeted ASO treatment at 30 nM ($n = 6$ independent biological replicates, Mean ± SEM, unpaired *t*-test, $^{*}p < 0.05$, $^{**}p < 0.01$, $^{***}p < 0.001$, $^{****}p < 0.0001$). (i) Experimental setup phagocytosis assay. (j) Phagocytosis of TAMRA-labeled Amyloid-β (Aβ) by THP-1 cells that were treated with human ASO2 or a matching scrambled control at 30 nM for 48 h ($n = 7$ independent biological replicates, Mean ± SEM, unpaired *t*-test, $^{*}p < 0.05$, $^{**}p < 0.01$, $^{***}p < 0.001$, $^{****}p < 0.0001$). (NOS2, nitric oxide synthase 2; Arg-1, arginase-1; Scr. Con. 3, scrambled control 3; MM Con. 3, mismatched control 3; Scr. Con. 2, scrambled control 2).

state (Heneka et al., 2013). Microglial immune activation is associated with an increased release of pro-inflammatory cytokines including TNF-α, IL-1β, IL-6, IL-12, and IL-18. In contrast, the anti-inflammatory phenotypes of microglia are associated with the release of IL-4, IL-10, IL-13, and TGF-β, and an increased phagocytic capacity (Heneka, Carson, et al., 2015; Mantovani et al., 2004). Our work reveals that NLRP3-targeted ASO treatment in primary murine microglia and human THP-1 cells can shift the cellular phenotypes toward a more anti-inflammatory state, as reflected by a downregulation of NOS2 and upregulation of arginase-1 mRNA levels.

In the brain, microglial cells play a major role in the detection, internalization, and degradation of Aβ (Lee & Landreth, 2010). This process is mediated by cell-surface receptors including CD36, CD14, α6β1 integrin, CD47, scavenger, and toll-like receptors (TLRs) (Bamberger et al., 2003; Heneka, Carson, et al., 2015; Liu et al., 2005; Paresce et al., 1996). However, binding of Aβ to CD36, TLR4, and TLR6 activates microglia, leading to the release of pro-inflammatory cytokines (El Khoury et al., 2003; Stewart et al., 2010). A co-culturing model of brain slices from APP/PS1 and wild-type mice has highlighted the role of CD68-positive microglial cells that clustered around amyloid plaques, and reduced the amyloid burden by phagocytosis of fibrillar Aβ deposits (Daria et al., 2017). Indeed, we were able to show that NLRP3-targeted ASO treatment increased the phagocytic profile of murine microglia or differentiated THP-1 cells, which was investigated using the mRNA levels of CD68 as a cellular marker. In both models, NLRP3-targeted ASO treatment significantly increased CD68 mRNA (Figure 6a,f). In the THP-1 cells, these mRNA changes were paralleled by a modest, but consistent, increase in Aβ phagocytosis (Figure 6j).

If the ASO-induced NLRP3 reduction can maintain increased Aβ clearance over longer periods of time, this may be harnessed to limit Aβ pathology in vivo. ASO-based approaches have already been approved for clinical use by both the European Medicines Agency (EMA) and the US Food and Drug Administration (FDA) for two drugs—nusinersen and inotersen—to treat the neurodegenerative diseases spinal muscular atrophy (SMA) and familial amyloid polyneuropathy and cardiomyopathy. These two ASOs contain the same chemical backbone modifications as used in our current study,

so the safety of such 'gapmer' oligonucleotides in patients is already well established (Bennett et al., 2021; Rinaldi & Wood, 2018). Nevertheless, there is still potential to improve the efficacy of the ASOs used in the present experiments. Key factors affecting ASO efficiency include degradation by nucleases, poor cellular uptake, and mRNA binding affinity (Shen & Corey, 2018). To improve these, other chemical modifications of the backbone may be required, such as phosphorodiamidate morpholino oligomers (PMO), which are resistant to nuclease and protease degradation (Bennett et al., 2021; Rinaldi & Wood, 2018). ASOs can also be designed to have an intrinsic enzymatic activity and directly cleave the target RNA after hybridization or they can prevent mRNA translation by altering ribosome recruitment (Rinaldi & Wood, 2018). In addition to these, passing the blood–brain barrier remains a major challenge of many therapies for neurodegenerative diseases (Mangan et al., 2018), but as shown for nusinersen, intrathecal injection of ASOs is a promising and effective route of administration (Haché et al., 2016).

The NLRP3 inflammasome acts as a key driver of chronic inflammatory conditions in a variety of diseases besides AD. These can be classified in four broad categories: first, genetic NLRP3-dependent autoinflammatory diseases; second, diseases driven by metabolic dysfunction; third, those driven by formation of crystals or aggregates; and fourth, fibrosis following either acute tissue injury or chronic inflammation (Mangan et al., 2018). These diseases include atherosclerosis, non-alcoholic fatty liver disease and non-alcoholic steatohepatitis (NASH), type 1 diabetes, myocardial infarction, and stroke (Duewell et al., 2010; Ito et al., 2015; Sandanger et al., 2013; Wree et al., 2014), and are among the top 10 causes of death worldwide (WHO, 2020). For all these conditions, it has been shown that NLRP3 deficiency or inhibition leads to an improvement in the respective pathology (Hu et al., 2015; Mridha et al., 2017; van der Heijden et al., 2017; van Hout et al., 2017; Yang et al., 2014). Together, our data shows that NLRP3-directed ASOs successfully suppresses the mRNA and protein levels of NLRP3, thus preventing assembly of the NLRP3 inflammasome and subsequent pro-inflammatory reactions. ASOs thus represent a fundamentally novel therapeutic strategy, not only for AD, but for multiple diseases associated with the NLRP3 inflammasome.

AUTHOR CONTRIBUTIONS

R.M.M. and M.T.H. contributed to the conceptualization and supervision. C.B., R.M.M., and M.T.H. contributed to the methodology. R.M.M. and C.B. contributed to the ASO design. C.B., M.P.K., K.A.R., M.G.d.F., A.G., S.S., and R.M.M. contributed to the investigation. C.B. and R.M.M. analyzed the data. C.B. and M.T.H. contributed to the writing—original draft. R.M.M. contributed to the writing—review and editing. R.M.M., M.T.H., C.B., and M.G.d.F. contributed to the funding acquisition.

ACKNOWLEDGMENTS

We thank I. Rácz for help with laboratory administration and S. Opitz and F. Santarelli for technical assistance. This work was funded by Deutscher Akademischer Austauschdienst, (Grant / Award Number: 'scholarship') Alzheimer Forschung Initiative, (Grant / Award Number: '20043') Deutsche Forschungsgemeinschaft, (Grant / Award Number: 'EXC2151 – 390873048 ') BONFOR research commission of the medical faculty of the University of Bonn, (Grant / Award Number: '2021-4-06'). Open Access funding enabled and organized by Projekt DEAL.

CONFLICT OF INTEREST STATEMENT

MTH is a former Editor for the Journal of Neurochemistry, and a clinical advisory board member at IFM Therapeutics, scientific advisory board member at Alector, honoraria for oral presentations from Pfizer, Novartis, Roche, Abbvie, NovoNordisk and Biogen. All other authors declare that they have no competing interests.

DATA AVAILABILITY STATEMENT

The data that support the findings of this study are available from the corresponding author upon reasonable request.

ORCID

Charlotte Braatz https://orcid.org/0000-0001-8490-5322
Kishore Aravind Ravichandran https://orcid.org/0000-0002-2429-5988
Matheus Garcia de Fragas https://orcid.org/0000-0002-5854-724X
Angelika Griep https://orcid.org/0000-0003-2568-9222
Róisín M. McManus https://orcid.org/0000-0002-6896-0302
Michael T. Heneka https://orcid.org/0000-0003-4996-1630

REFERENCES

Andreeva, L., David, L., Rawson, S., Shen, C., Pasricha, T., Pelegrin, P., & Wu, H. (2021). NLRP3 cages revealed by full-length mouse NLRP3 structure control pathway activation. *Cell*, *184*(26), 6299–6312. e22. https://doi.org/10.1016/j.cell.2021.11.011

Balon, K., & Wiatrak, B. (2021). PC12 and THP-1 cell lines as neuronal and microglia model in neurobiological research. *Applied Sciences*, *11*(9), 3729. https://doi.org/10.3390/app11093729

Bamberger, M. E., Harris, M. E., McDonald, D. R., Husemann, J., & Landreth, G. E. (2003). A cell surface receptor complex for Fibrillar β-amyloid mediates microglial activation. *The Journal of Neuroscience*, *23*(7), 2665–2674. https://doi.org/10.1523/JNEUROSCI.23-07-02665.2003

Bennett, C. F., Kordasiewicz, H. B., & Cleveland, D. W. (2021). Antisense drugs make sense for neurological diseases. *Annual Review of Pharmacology and Toxicology*, *61*(1), 831–852. https://doi.org/10.1146/annurev-pharmtox-010919-023738

Bennett, C. F., & Swayze, E. E. (2010). RNA targeting therapeutics: Molecular mechanisms of antisense oligonucleotides as a therapeutic platform. *Annual Review of Pharmacology and Toxicology*, *50*(1), 259–293. https://doi.org/10.1146/annurev.pharmtox.010909.105654

Boucher, D., Monteleone, M., Coll, R. C., Chen, K. W., Ross, C. M., Teo, J. L., Gomez, G. A., Holley, C. L., Bierschenk, D., Stacey, K. J., Yap, A. S., Bezbradica, J. S., & Schroder, K. (2018). Caspase-1 self-cleavage is an intrinsic mechanism to terminate inflammasome activity. *Journal of Experimental Medicine*, *215*(3), 827–840. https://doi.org/10.1084/jem.20172222

Crooke, S. T., Wang, S., Vickers, T. A., Shen, W., & Liang, X. (2017). Cellular uptake and trafficking of antisense oligonucleotides. *Nature Biotechnology*, *35*(3), 230–237. https://doi.org/10.1038/nbt.3779

Daria, A., Colombo, A., Llovera, G., Hampel, H., Willem, M., Liesz, A., Haass, C., & Tahirovic, S. (2017). Young microglia restore amyloid plaque clearance of aged microglia. *The EMBO Journal*, *36*(5), 583–603. https://doi.org/10.15252/embj.201694591

DeVos, S. L., Miller, R. L., Schoch, K. M., Holmes, B. B., Kebodeaux, C. S., Wegener, A. J., Chen, G., Shen, T., Tran, H., Nichols, B., Zanardi, T. A., Kordasiewicz, H. B., Swayze, E. E., Bennett, C. F., Diamond, M. I., & Miller, T. M. (2017). Tau reduction prevents neuronal loss and reverses pathological tau deposition and seeding in mice with tauopathy. *Science Translational Medicine*, *9*(374), eaag0481. https://doi.org/10.1126/scitranslmed.aag0481

Dinarello, C. A., Simon, A., & van der Meer, J. W. M. (2012). Treating inflammation by blocking interleukin-1 in a broad spectrum of diseases. *Nature Reviews Drug Discovery*, *11*(8), 633–652. https://doi.org/10.1038/nrd3800

Duewell, P., Kono, H., Rayner, K. J., Sirois, C. M., Vladimer, G., Bauernfeind, F. G., Abela, G. S., Franchi, L., Nuñez, G., Schnurr, M., Espevik, T., Lien, E., Fitzgerald, K. A., Rock, K. L., Moore, K. J., Wright, S. D., Hornung, V., & Latz, E. (2010). NLRP3 inflammasomes are required for atherogenesis and activated by cholesterol crystals. *Nature*, *464*(7293), 1357–1361. https://doi.org/10.1038/nature08938

El Khoury, J. B., Moore, K. J., Means, T. K., Leung, J., Terada, K., Toft, M., Freeman, M. W., & Luster, A. D. (2003). CD36 mediates the innate host response to β-amyloid. *Journal of Experimental Medicine*, *197*(12), 1657–1666. https://doi.org/10.1084/jem.20021546

Gagnon, K. T., & Corey, D. R. (2019). Guidelines for experiments using antisense oligonucleotides and double-stranded RNAs. *Nucleic Acid Therapeutics*, *29*(3), 116–122. https://doi.org/10.1089/nat.2018.0772

Gauthier, S., Rosa-Neto, P., Morais, J. A., & Webster, C. (2021). *World Alzheimer report 2021: Journey through the diagnosis of dementia*. Alzheimer's Disease International. https://www.alzint.org/u/World-Alzheimer-Report-2021.pdf

Giordano, G., Hong, S., Faustman, E. M., & Costa, L. G. (2011). Measurements of cell death in neuronal and glial cells. In L. G. Costa, G. Giordano, & M. Guizzetti (Eds.), (Hrsg.) *Vitro Neurotoxicology* (Vol. *Bd. 758*, pp. 171–178). Humana Press. https://doi.org/10.1007/978-1-61779-170-3_11

Haché, M., Swoboda, K. J., Sethna, N., Farrow-Gillespie, A., Khandji, A., Xia, S., & Bishop, K. M. (2016). Intrathecal injections in children with spinal muscular atrophy: Nusinersen clinical trial experience. *Journal of Child Neurology*, *31*(7), 899–906. https://doi.org/10.1177/0883073815627882

Halle, A., Hornung, V., Petzold, G. C., Stewart, C. R., Monks, B. G., Reinheckel, T., Fitzgerald, K. A., Latz, E., Moore, K. J., & Golenbock, D. T. (2008). The NALP3 inflammasome is involved in the innate immune response to amyloid-β. *Nature Immunology*, *9*(8), Art. 8–Art. 865. https://doi.org/10.1038/ni.1636

Heneka, M. T., Carson, M. J., Khoury, J. E., Landreth, G. E., Brosseron, F., Feinstein, D. L., Jacobs, A. H., Wyss-Coray, T., Vitorica, J., Ransohoff, R. M., Herrup, K., Frautschy, S. A., Finsen, B., Brown, G. C., Verkhratsky, A., Yamanaka, K., Koistinaho, J., Latz, E., Halle, A., … Kummer, M. P. (2015). Neuroinflammation in Alzheimer's disease. *The Lancet Neurology*, *14*(4), 388–405. https://doi.org/10.1016/S1474-4422(15)70016-5

Heneka, M. T., Golenbock, D. T., & Latz, E. (2015). Innate immunity in Alzheimer's disease. *Nature Immunology*, *16*(3), 229–236. https://doi.org/10.1038/ni.3102

Heneka, M. T., Kummer, M. P., & Latz, E. (2014). Innate immune activation in neurodegenerative disease. *Nature Reviews Immunology*, *14*(7), 7. https://doi.org/10.1038/nri3705

Heneka, M. T., Kummer, M. P., Stutz, A., Delekate, A., Schwartz, S., Vieira-Saecker, A., Griep, A., Axt, D., Remus, A., Tzeng, T.-C., Gelpi, E., Halle, A., Korte, M., Latz, E., & Golenbock, D. T. (2013). NLRP3 is activated in Alzheimer's disease and contributes to pathology in APP/PS1 mice. *Nature*, *493*(7434), 678. https://doi.org/10.1038/nature11729

Heneka, M. T., McManus, R. M., & Latz, E. (2018). Inflammasome signalling in brain function and neurodegenerative disease. *Nature Reviews Neuroscience*, *19*(10), 610–621. https://doi.org/10.1038/s41583-018-0055-7

Hochheiser, I. V., Pilsl, M., Hagelueken, G., Moecking, J., Marleaux, M., Brinkschulte, R., Latz, E., Engel, C., & Geyer, M. (2022). Structure of the NLRP3 decamer bound to the cytokine release inhibitor CRID3. *Nature*, *604*(7904), 184–189. https://doi.org/10.1038/s41586-022-04467-w

Hu, C., Ding, H., Li, Y., Pearson, J. A., Zhang, X., Flavell, R. A., Wong, F. S., & Wen, L. (2015). NLRP3 deficiency protects from type 1 diabetes through the regulation of chemotaxis into the pancreatic islets. *Proceedings of the National Academy of Sciences*, *112*(36), 11318–11323. https://doi.org/10.1073/pnas.1513509112

Ising, C., Venegas, C., Zhang, S., Scheiblich, H., Schmidt, S. V., Vieira-Saecker, A., Schwartz, S., Albasset, S., McManus, R. M., Tejera, D., Griep, A., Santarelli, F., Brosseron, F., Opitz, S., Stunden, J., Merten, M., Kayed, R., Golenbock, D. T., Blum, D., … Heneka, M. T. (2019). NLRP3 inflammasome activation drives tau pathology. *Nature*, *575*(7784), 669–673. https://doi.org/10.1038/s41586-019-1769-z

Ito, M., Shichita, T., Okada, M., Komine, R., Noguchi, Y., Yoshimura, A., & Morita, R. (2015). Bruton's tyrosine kinase is essential for NLRP3 inflammasome activation and contributes to ischaemic brain injury. *Nature Communications*, *6*(1), 7360. https://doi.org/10.1038/ncomms8360

Jankowsky, J. L., Slunt, H. H., Ratovitski, T., Jenkins, N. A., Copeland, N. G., & Borchelt, D. R. (2001). Co-expression of multiple transgenes in mouse CNS: A comparison of strategies. *Biomolecular Engineering*, *17*(6), 157–165. https://doi.org/10.1016/S1389-0344(01)00067-3

Kummer, M. P., Hermes, M., Delekarte, A., Hammerschmidt, T., Kumar, S., Terwel, D., Walter, J., Pape, H.-C., König, S., Roeber, S., Jessen, F., Klockgether, T., Korte, M., & Heneka, M. T. (2011). Nitration of tyrosine 10 critically enhances amyloid β aggregation and plaque formation. *Neuron*, *71*(5), 833–844. https://doi.org/10.1016/j.neuron.2011.07.001

Latz, E., Xiao, T. S., & Stutz, A. (2013). Activation and regulation of the inflammasomes. *Nature Reviews Immunology*, *13*(6), 397–411. https://doi.org/10.1038/nri3452

Lee, C. Y. D., & Landreth, G. E. (2010). The role of microglia in amyloid clearance from the AD brain. *Journal of Neural Transmission*, *117*(8), 949–960. https://doi.org/10.1007/s00702-010-0433-4

Liu, Y., Walter, S., Stagi, M., Cherny, D., Letiembre, M., Schulz-Schaeffer, W., Heine, H., Penke, B., Neumann, H., & Fassbender, K. (2005). LPS receptor (CD14): A receptor for phagocytosis of Alzheimer's amyloid peptide. *Brain*, *128*(8), 1778–1789. https://doi.org/10.1093/brain/awh531

Lučiūnaitė, A., McManus, R. M., Jankunec, M., Rácz, I., Dansokho, C., Dalgėdienė, I., Schwartz, S., Brosseron, F., & Heneka, M. T. (2020). Soluble Aβ oligomers and protofibrils induce NLRP3 inflammasome activation in microglia. *Journal of Neurochemistry*, *155*(6), 650–661. https://doi.org/10.1111/jnc.14945

Mangan, M. S. J., Olhava, E. J., Roush, W. R., Seidel, H. M., Glick, G. D., & Latz, E. (2018). Targeting the NLRP3 inflammasome in inflammatory diseases. *Nature Reviews Drug Discovery*, *17*(8), 588–606. https://doi.org/10.1038/nrd.2018.97

Mantovani, A., Sica, A., Sozzani, S., Allavena, P., Vecchi, A., & Locati, M. (2004). The chemokine system in diverse forms of macrophage activation and polarization. *Trends in Immunology*, *25*(12), 677–686. https://doi.org/10.1016/j.it.2004.09.015

Martinon, F., Burns, K., & Tschopp, J. (2002). The inflammasome. *Molecular Cell*, *10*(2), 417–426. https://doi.org/10.1016/S1097-2765(02)00599-3

Mawuenyega, K. G., Sigurdson, W., Ovod, V., Munsell, L., Kasten, T., Morris, J. C., Yarasheski, K. E., & Bateman, R. J. (2010). Decreased clearance of CNS β-amyloid in Alzheimer's disease. *Science*, *330*(6012), 1774. https://doi.org/10.1126/science.1197623

Mridha, A. R., Wree, A., Robertson, A. A. B., Yeh, M. M., Johnson, C. D., Van Rooyen, D. M., Haczeyni, F., Teoh, N. C.-H., Savard, C., Ioannou, G. N., Masters, S. L., Schroder, K., Cooper, M. A., Feldstein, A. E., & Farrell, G. C. (2017). NLRP3 inflammasome blockade reduces

liver inflammation and fibrosis in experimental NASH in mice. *Journal of Hepatology*, *66*(5), 1037–1046. https://doi.org/10.1016/j.jhep.2017.01.022

Paolicelli, R. C., Sierra, A., Stevens, B., Tremblay, M. E., Aguzzi, A., Ajami, B., Amit, I., Audinat, E., Bechmann, I., Bennett, M., Bennett, F., Bessis, A., Biber, K., Bilbo, S., Blurton-Jones, M., Boddeke, E., Brites, D., Brône, B., Brown, G. C., … Wyss-Coray, T. (2022). Microglia states and nomenclature: A field at its crossroads. *Neuron*, *110*, 3458–3483.

Paresce, D. M., Ghosh, R. N., & Maxfield, F. R. (1996). Microglial cells internalize aggregates of the Alzheimer's disease amyloid β-protein via a scavenger receptor. *Neuron*, *17*(3), 553–565. https://doi.org/10.1016/S0896-6273(00)80187-7

Patil, S. D., Rhodes, D. G., & Burgess, D. J. (2005). DNA-based therapeutics and DNA delivery systems: A comprehensive review. *The AAPS Journal*, *7*(1), E61–E77. https://doi.org/10.1208/aapsj070109

Pétrilli, V., Papin, S., Dostert, C., Mayor, A., Martinon, F., & Tschopp, J. (2007). Activation of the NALP3 inflammasome is triggered by low intracellular potassium concentration. *Cell Death & Differentiation*, *14*(9), 1583–1589. https://doi.org/10.1038/sj.cdd.4402195

Raes, L., Pille, M., Harizaj, A., Goetgeluk, G., Van Hoeck, J., Stremersch, S., Fraire, J. C., Brans, T., de Jong, O. G., Maas-Bakker, R., Mastrobattista, E., Vader, P., De Smedt, S. C., Vandekerckhove, B., Raemdonck, K., & Braeckmans, K. (2021). Cas9 RNP transfection by vapor nanobubble photoporation for ex vivo cell engineering. *Molecular Therapy—Nucleic Acids*, *25*, 696–707. https://doi.org/10.1016/j.omtn.2021.08.014

Rathinam, V. A. K., Zhao, Y., & Shao, F. (2019). Innate immunity to intracellular LPS. *Nature Immunology*, *20*(5), 527–533. https://doi.org/10.1038/s41590-019-0368-3

Reitz, C., & Mayeux, R. (2014). Alzheimer disease: Epidemiology, diagnostic criteria, risk factors and biomarkers. *Biochemical Pharmacology*, *88*(4), 640–651. https://doi.org/10.1016/j.bcp.2013.12.024

Rinaldi, C., & Wood, M. J. A. (2018). Antisense oligonucleotides: The next frontier for treatment of neurological disorders. *Nature Reviews Neurology*, *14*(1), 1. https://doi.org/10.1038/nrneurol.2017.148

Sandanger, Ø., Ranheim, T., Vinge, L. E., Bliksøen, M., Alfsnes, K., Finsen, A. V., Dahl, C. P., Askevold, E. T., Florholmen, G., Christensen, G., Fitzgerald, K. A., Lien, E., Valen, G., Espevik, T., Aukrust, P., & Yndestad, A. (2013). The NLRP3 inflammasome is up-regulated in cardiac fibroblasts and mediates myocardial ischaemia–reperfusion injury. *Cardiovascular Research*, *99*(1), 164–174. https://doi.org/10.1093/cvr/cvt091

Scharner, J., & Aznarez, I. (2021). Clinical applications of single-stranded oligonucleotides: Current landscape of approved and In-development therapeutics. *Molecular Therapy*, *29*(2), 540–554. https://doi.org/10.1016/j.ymthe.2020.12.022

Schnaars, M., Beckert, H., & Halle, A. (2013). Assessing β-amyloid-induced NLRP3 Inflammasome activation in primary microglia. In De Nardo C. M. & E. Latz (Hrsg.), *The Inflammasome* (Bd. *1040*, 1–8). Humana Press. https://doi.org/10.1007/978-1-62703-523-1_1

Schoch, K. M., DeVos, S. L., Miller, R. L., Chun, S. J., Norrbom, M., Wozniak, D. F., Dawson, H. N., Bennett, C. F., Rigo, F., & Miller, T. M. (2016). Increased 4R-tau induces pathological changes in a human-tau mouse model. *Neuron*, *90*(5), 941–947. https://doi.org/10.1016/j.neuron.2016.04.042

Shen, X., & Corey, D. R. (2018). Chemistry, mechanism and clinical status of antisense oligonucleotides and duplex RNAs. *Nucleic Acids Research*, *46*(4), 1584–1600. https://doi.org/10.1093/nar/gkx1239

Stewart, C. R., Stuart, L. M., Wilkinson, K., van Gils, J. M., Deng, J., Halle, A., Rayner, K. J., Boyer, L., Zhong, R., Frazier, W. A., Lacy-Hulbert, A., Khoury, J. E., Golenbock, D. T., & Moore, K. J. (2010). CD36 ligands promote sterile inflammation through assembly of a toll-like receptor 4 and 6 heterodimer. *Nature Immunology*, *11*(2), 155–161. https://doi.org/10.1038/ni.1836

Sud, R., Geller, E. T., & Schellenberg, G. D. (2014). Antisense-mediated exon skipping decreases tau protein expression: A potential therapy for Tauopathies. *Molecular Therapy—Nucleic Acids*, *3*, e180. https://doi.org/10.1038/mtna.2014.30

van der Heijden, T., Kritikou, E., Venema, W., van Duijn, J., van Santbrink, P. J., Slütter, B., Foks, A. C., Bot, I., & Kuiper, J. (2017). NLRP3 Inflammasome Inhibition by MCC950 Reduces Atherosclerotic Lesion Development in Apolipoprotein E–Deficient Mice—Brief Report. *Arteriosclerosis, Thrombosis, and Vascular Biology*, *37*(8), 1457–1461. https://doi.org/10.1161/ATVBAHA.117.309575

van Hout, G. P. J., Bosch, L., Ellenbroek, G. H. J. M., de Haan, J. J., van Solinge, W. W., Cooper, M. A., Arslan, F., de Jager, S. C. A., Robertson, A. A. B., Pasterkamp, G., & Hoefer, I. E. (2017). The selective NLRP3-inflammasome inhibitor MCC950 reduces infarct size and preserves cardiac function in a pig model of myocardial infarction. *European Heart Journal*, *38*(11), 828–836. https://doi.org/10.1093/eurheartj/ehw247

Venegas, C., Kumar, S., Franklin, B. S., Dierkes, T., Brinkschulte, R., Tejera, D., Vieira-Saecker, A., Schwartz, S., Santarelli, F., Kummer, M. P., Griep, A., Gelpi, E., Beilharz, M., Riedel, D., Golenbock, D. T., Geyer, M., Walter, J., Latz, E., & Heneka, M. T. (2017). Microglia-derived ASC specks cross-seed amyloid-β in Alzheimer's disease. *Nature*, *552*(7685), 355–361. https://doi.org/10.1038/nature25158

Weiner, H. L., & Frenkel, D. (2006). Immunology and immunotherapy of Alzheimer's disease. *Nature Reviews Immunology*, *6*(5), 5. https://doi.org/10.1038/nri1843

WHO. (2020). *The top 10 causes of death*. https://www.who.int/news-room/fact-sheets/detail/the-top-10-causes-of-death

Wree, A., McGeough, M. D., Peña, C. A., Schlattjan, M., Li, H., Inzaugarat, M. E., Messer, K., Canbay, A., Hoffman, H. M., & Feldstein, A. E. (2014). NLRP3 inflammasome activation is required for fibrosis development in NAFLD. *Journal of Molecular Medicine*, *92*(10), 1069–1082. https://doi.org/10.1007/s00109-014-1170-1

Yamanaka, M., Ishikawa, T., Griep, A., Axt, D., Kummer, M. P., & Heneka, M. T. (2012). PPAR/RXR -induced and CD36-mediated microglial amyloid- phagocytosis results in cognitive improvement in amyloid precursor protein/Presenilin 1 mice. *Journal of Neuroscience*, *32*(48), 17321–17331. https://doi.org/10.1523/JNEUROSCI.1569-12.2012

Yang, F., Wang, Z., Wei, X., Han, H., Meng, X., Zhang, Y., Shi, W., Li, F., Xin, T., Pang, Q., & Yi, F. (2014). NLRP3 deficiency ameliorates neurovascular damage in experimental ischemic stroke. *Journal of Cerebral Blood Flow & Metabolism*, *34*(4), 660–667. https://doi.org/10.1038/jcbfm.2013.242

SUPPORTING INFORMATION

Additional supporting information can be found online in the Supporting Information section at the end of this article.

How to cite this article: Braatz, C., Komes, M. P., Ravichandran, K. A., de Fragas, M. G., Griep, A., Schwartz, S., McManus, R. M., & Heneka, M. T. (2024). NLRP3-directed antisense oligonucleotides reduce microglial immunoactivities in vitro. *Journal of Neurochemistry*, *168*, 3467–3481. https://doi.org/10.1111/jnc.15778